

Figure 6.1: Average aperture number density ($\bar{\rho}_{250}$) vs look back time for X-ray detected active galaxies (left) and variability detected active galaxies (right). X-ray bright active galaxies are denoted by blue crosses, variability detected active galaxies are shown as red points and corresponding matched control galaxies are shown as black points. Galaxies are averaged in bins of 2Gyrs, with error bars in grey representing the standard error on the mean. Look back times are calculated based on the measured redshift and the cosmology quoted in the Introduction (Chapter 1) and corresponding redshifts are shown on the top x-axis of the plot. $\langle \Delta \bar{\rho}_{250} \rangle$ denotes the difference in the overall mean ρ_{250} for all epochs between the active galaxies and their corresponding control galaxies.

taking into account masking and the edges of the field, to give the value of relative density. This density, ρ_{250} , is the environmental density measure we make use of in this analysis, with values greater than one indicating an over-dense region and values less than one indicating an under-dense region.

6.5 Results

6.5.1 Environment

To investigate if and how observations of active galaxies differ from inactive galaxies, we first examine the large scale properties by studying the environment the galaxies reside in. Using the full ground-based UDS sample, in Figure 6.1 we plot the aperture number density vs look back time for the X-ray bright and variability-detected active galaxies and corresponding matched control galaxies. Inspecting this figure, we find both X-ray bright and variability detected active galaxies are found in different environments compared to their matched control galaxies. In the X-ray sample, active and control galaxies follow

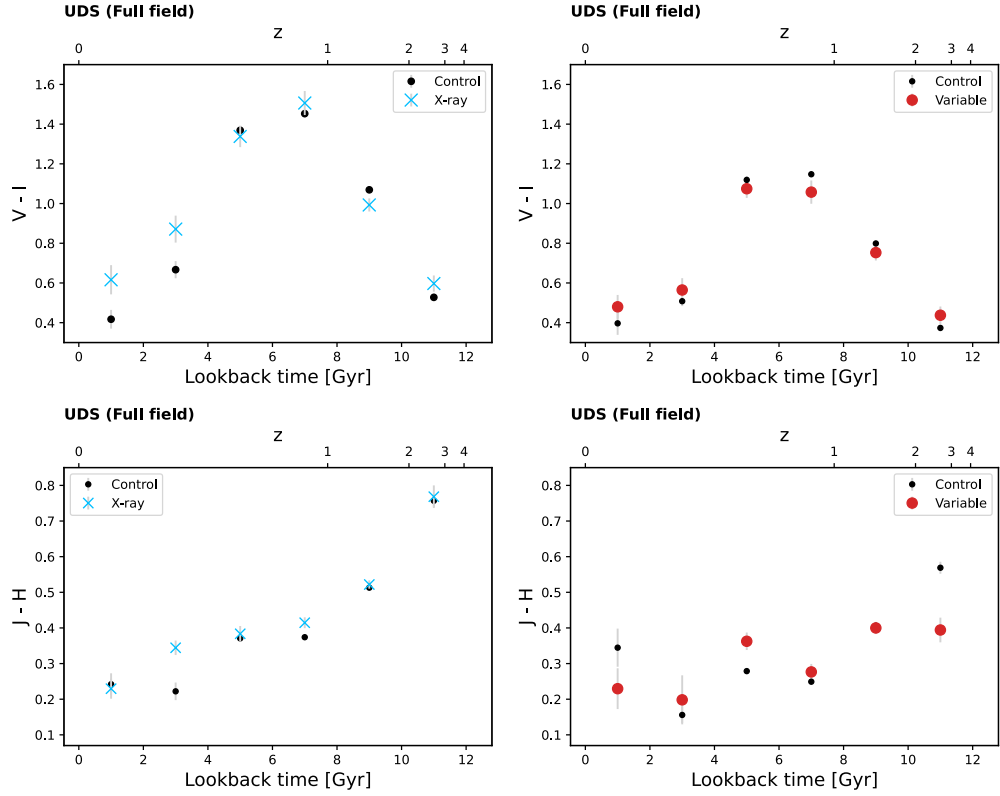


Figure 6.2: Optical $V - I$ (top) and infrared $J - H$ (bottom) colour vs look back time for active galaxies and their matched control galaxies. The left column shows X-ray detected AGN as blue crosses and the right column shows variability detected active galaxies as red points. In both groups corresponding control galaxies are black points. Galaxies in these samples are drawn from the full, ground-based UDS field and measured magnitudes are apparent magnitudes. Galaxy colours are averaged in bins of 2Gyrs with error bars being the standard error on the mean. Look back times are calculated based on the redshift, and corresponding redshifts are shown on the top x-axis of the plots.

similar distributions across cosmic time, but active galaxies are consistently found in denser environments compared to the control galaxies for all epochs studied. This result is in agreement with previous work studying the environments of X-ray bright active galaxies, which found AGN to reside in overdense environments (e.g. Bradshaw et al., 2011). Active and control galaxies in the variability detected sample however show no obvious similarities in the evolution of their environment. Instead, the variability detected sample seems to show no obvious connection to their environment across cosmic time, whereas the matched control sample shows an evolution akin to the X-ray detected sample, with the average environmental density increasing until ~ 5 Gyrs and then decreasing beyond this value.

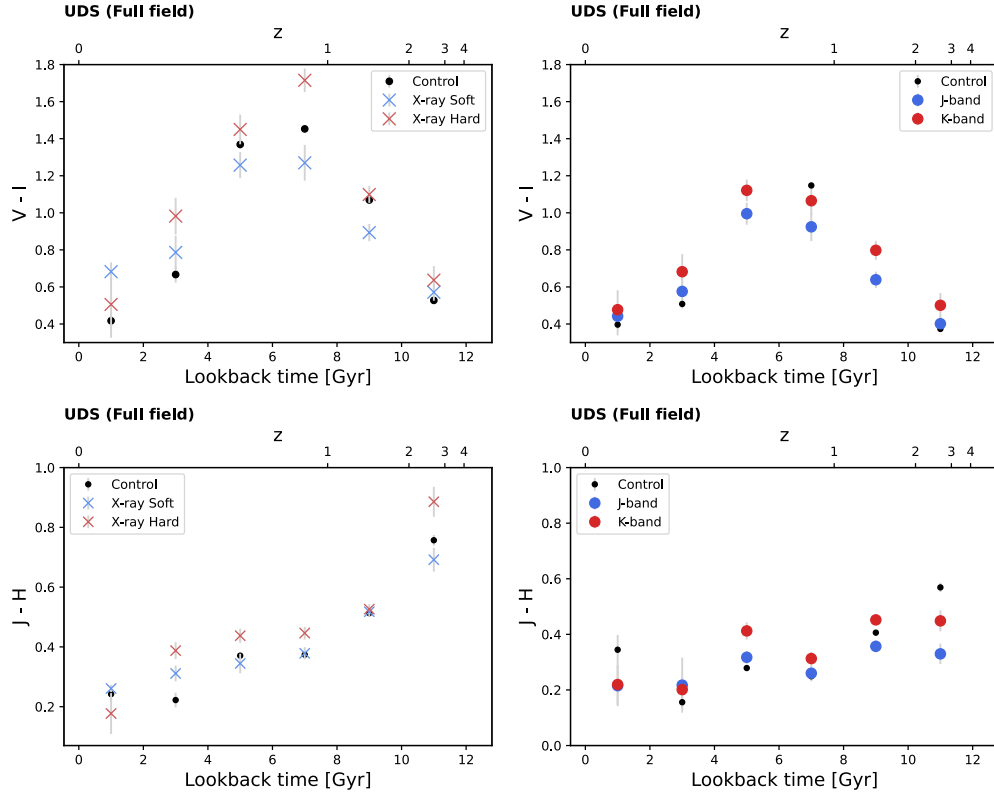


Figure 6.3: Optical ($V - I$, top) and infrared ($J - H$, bottom) colour vs look back time for active galaxies and their matched control galaxies. Galaxies in these samples are drawn from the full, ground-based UDS field and measured magnitudes are apparent magnitudes. X-ray bright samples are shown as crosses and are split based on hardness ratio, with X-ray soft ($HR < 0$) in blue and X-ray hard ($HR \geq 0$) in red. Significantly variable galaxies are denoted by coloured points, with any active galaxy variable in the J -band in blue and any active galaxy variable in the K -band in red. In both samples control galaxies are matched to the overall active populations and are denoted as black points. Galaxy colours are averaged in bins of 2 Gyrs with error bars being the standard error on the mean. Look back times are calculated based on the redshift, and corresponding redshifts are shown on the top x-axis of the plots.

6.5.2 Infrared and optical colour comparisons

Having studied the wider environments of active galaxies, we next inspect the features of the galaxies themselves. One interesting property to study is if AGN emission has a significant impact on the observed colours of active galaxies. Again, investigating the ground-based UDS field by using apparent magnitude measurements of the active galaxies as a whole, we plot the optical $V - I$ and infrared $J - H$ colour as a function

of cosmic time in Figure 6.2. Here we find that both X-ray bright and variability-detected active galaxies appear to have similar colours compared to control galaxies, with this holding for all epochs studied. However, comparing the X-ray and variability detected groups to each other does find noticeable differences. In the optical ($V - I$) colour, we probe the 4000\AA break at ≈ 1 , and in the infrared ($J - H$) the 4000\AA break occurs at ≈ 2 . In both colours, the X-ray samples appear redder than the variability detected samples, and one explanation for this could be due to the X-ray bright sample preferentially selecting AGN in massive galaxies, which tend to have higher passive fractions. This explanation is supported by the control galaxies matched to the X-ray bright sample showing similar results, and suggests that variability detected AGN are a stochastic process that can be found in a wide range of galaxies.

To see if active galaxies as a global population have comparable colours to inactive galaxies, we further investigate the colour evolution of the samples by splitting the galaxies into subgroups. X-ray detected galaxies are measured in the full band (0.5-10keV) and are split based on hardness ratio into X-ray soft ($HR < 0$) and X-ray hard ($HR \geq 0$) galaxies, and variability detected galaxies are split based on J and K -band variability. Plotting the optical and infrared colours of these galaxies against look back time in Figure 6.3, differences appear in the samples, with the colours of the subgroups being consistently offset from each other. X-ray hard galaxies are consistently redder than X-ray soft galaxies except in the lowest redshift bin, and K -band variable galaxies appear redder in both optical and infrared colours compared to their J -band variable counterparts. Inspecting the 4000\AA break at ≈ 1 in the optical and at ≈ 2 in the infrared, we note that the magnitude of the colour difference between X-ray hard and X-ray soft galaxies increases compared to measurements at other redshifts; which would occur if X-ray hard galaxies do preferentially probe more evolved stellar systems. Colour differences between J and K -band variable AGN remain largely consistent throughout cosmic time, which provides further evidence in support of K -band variable AGN residing in dusty galaxies, as explored in Chapter 5.

Having studied the wider environment and average properties of active galaxies across cosmic time, we next inspect the individual properties of the active galaxies by comparing the colour evolution for a given galaxy morphological type. In Figure 6.4, we again plot the optical ($V - I$) and infrared ($J - H$) colour vs look back time, however we split the sample into disk-types and spheroids based on the Sérsic index n as a measure of morphology. First, examining the disk-type galaxies, we find that X-ray bright active

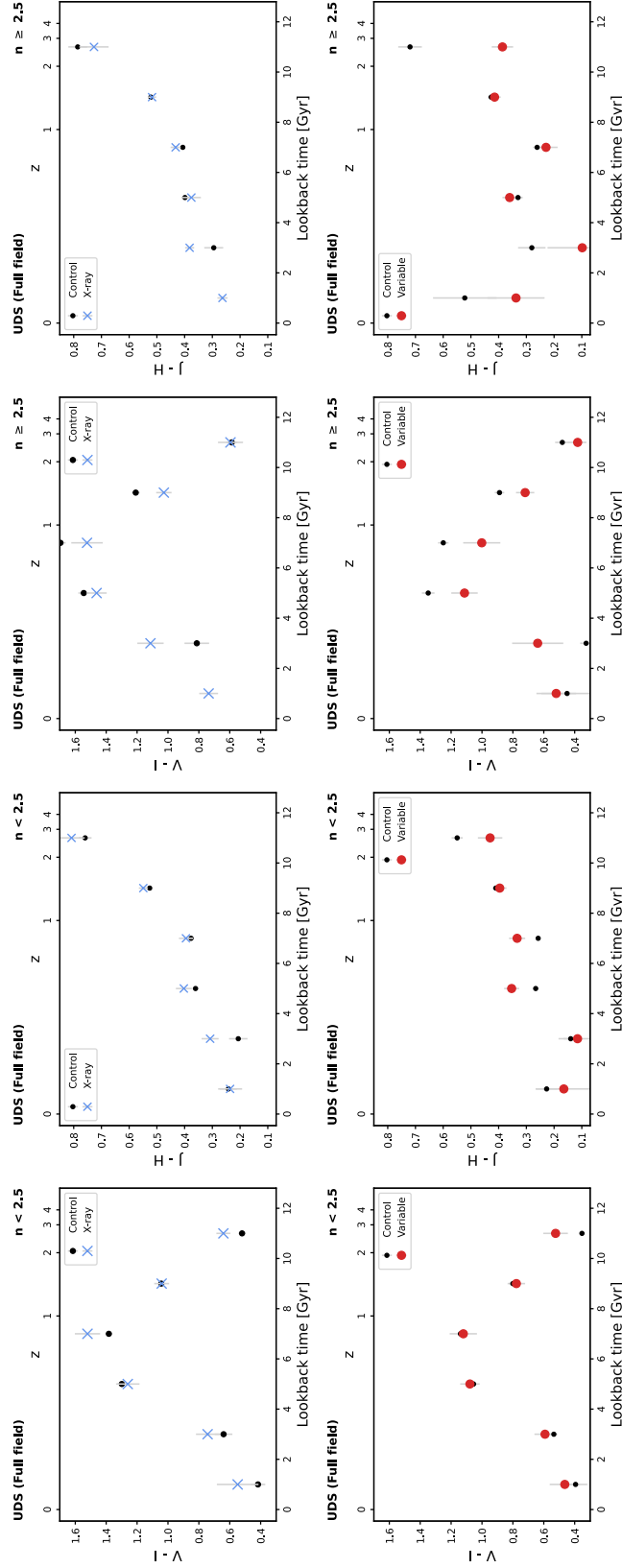


Figure 6.4: Optical $V - I$ and infrared $J - H$ colour vs look back time for X-ray bright (top) and infrared variable (bottom) active galaxies and matched control galaxies. Galaxies are split based on their Sérsic index (n) as a morphology measure, with disk type galaxies ($n < 2.5$) in the first two columns and spheroidal galaxies ($n \geq 2.5$) in the third and fourth columns. X-ray detected AGN are shown as blue crosses and variability detected active galaxies are denoted by red points; in both groups corresponding control galaxies are black points. Galaxy colours are averaged in bins of 2Gyrs with error bars being the standard error on the mean. Galaxies in these samples are drawn from the full, ground-based UDS field, measured magnitudes and Sérsic indices are measured on ground-based, K -band imaging.

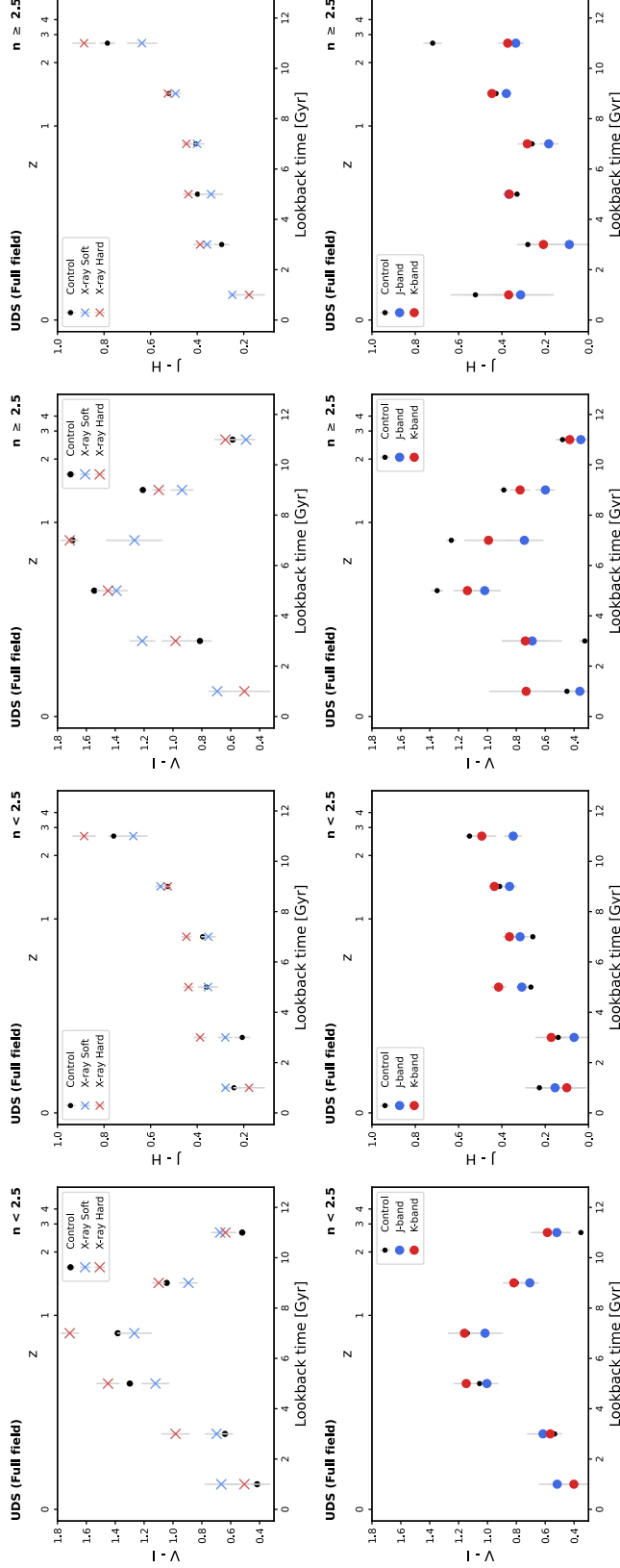


Figure 6.5: Optical ($V - I$) and infrared ($J - H$) colour vs look back time for X-ray bright (top) and infrared variable (bottom) active galaxies and matched control galaxies. Galaxies are split based on their Sérsic index (n) as a morphology measure, with disk type galaxies ($n < 2.5$) in the first two columns and spheroidal galaxies ($n \geq 2.5$) in the third and fourth columns. X-ray bright samples are shown as crosses and split based on hardness ratio, with X-ray soft ($HR < 0$) in blue and X-ray hard ($HR \geq 0$) in red. Significantly variable galaxies are denoted by coloured circles, with any active galaxy variable in the J -band in blue and any active galaxy variable in the K -band in red. In both samples control galaxies are matched to the overall active populations and are denoted as black points. Galaxy colours are averaged in bins of 2Gyrs with error bars being the standard error on the mean. Galaxies in these samples are drawn from the full, ground-based UDS field, measured magnitudes and Sérsic indices are measured on ground-based, K -band imaging.

galaxies appear slightly redder in both optical and IR colours compared to matched control galaxies across cosmic time, whereas variability detected active galaxies have similar infrared and optical colours compared to control galaxies across the redshift range probed in this study. Considering the spheroidal sample finds more pronounced differences; both X-ray bright and variability detected active galaxies show redder optical colours compared to control galaxies at lower look back times, but as look back times increase active galaxies appear bluer compared to control galaxies, opposite to what is observed in the more local Universe. In contrast to the similar colour distributions between spheroidal X-ray and variability detected AGN in the optical, X-ray and variability detected active galaxies show different infrared colour evolutions. Spheroidal X-ray bright active galaxies and their matched control galaxies have largely similar infrared across cosmic time, but spheroidal variability detected active galaxies show no obvious correlation with infrared colour compared to their control galaxies at a given epoch.

Following the differences found when investigating how the colours of active galaxies, split by morphological type, change over cosmic time, we create further subgroups for analysis by categorising the galaxies by X-ray hardness ratio and variability band. This separation is shown in Figure 6.5 where, for a given morphological type at a given redshift bin, a vast majority of X-ray hard galaxies are redder in both optical and infrared colour than X-ray soft galaxies, and *K*-band variable galaxies are redder in optical and infrared colours than *J*-band variable galaxies. We also find that the magnitude of the colour difference between X-ray subgroups increases at the 4000Å break, whereas colour differences are generally consistent when comparing variable subgroups, in agreement with the observations in Figure 6.3.

6.5.3 Two component Sérsic point source fits

In Section 6.5.2, we studied the conditions and extent by which observations of active galaxies differ to those of inactive galaxies. However, to be able to gather accurate properties of the galaxies AGN exist in, AGN and host galaxy emission must be separated out. To remove AGN contamination on host galaxy emission, we perform a two component fit to active galaxy imaging, where a point source component is included to account for AGN radiation and a standard Sérsic profile is used to calculate host

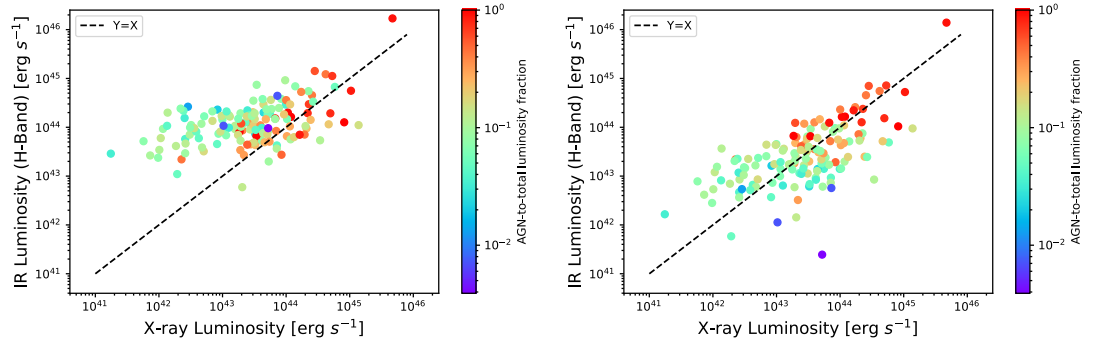


Figure 6.6: H -band infrared luminosity vs full band (0.5-10keV) X-ray luminosity for the X-ray detected active galaxies found within the CANDELS-UDS imaging region. In the left plot the infrared luminosity is based on a single Sérsic fit to the galaxy image, in the right plot the infrared luminosity is calculated from the magnitude returned from the PSF component in a combined Sérsic + PSF fit to the active galaxies. In both plots the X-ray luminosity is drawn from the Chandra X-ray catalogue (see Chapter 2). Points are colour coded according to the fraction of the total luminosity of the object attributed to the PSF component in the two component Sérsic + PSF fit. The black dashed line traces unity.

parameters.

To measure the host galaxy parameters, we use CANDELS-UDS optical and infrared imaging (Section 6.2.2) of a subsection of the wider UKIDSS UDS field. To determine the effectiveness of this approach, we examine how the X-ray luminosity compares to the infrared luminosity in Figure 6.6. According to AGN emission theory, a majority of the X-rays originate from the AGN in a given active galaxy. The SED of active galaxies is also largely flat between X-ray and infrared emission, and as such one would expect approximately equal IR luminosities and X-ray luminosities. Examining Figure 6.6, we find that a two component fit is required to accurately model the emission from active galaxies. A single Sérsic fit proves to be insufficient, and this is most apparent in galaxies where the AGN counts for $\lesssim 25\%$ of the total emission. In such galaxies, modelling the combined AGN and host galaxy emission via a single Sérsic profile results in an overestimation of the AGN radiation, however including a PSF component as a model for point-source AGN emission allows for the AGN emission to be separated out and credibly fitted in the analysis, causing measured luminosities to drop to more sensible values. Using a two component Sérsic + PSF fit to the active galaxies also allows for the fraction that the host galaxy and AGN contribute to the overall observed flux to be determined. Inspecting this, we find that the brighter the galaxy, the more the AGN

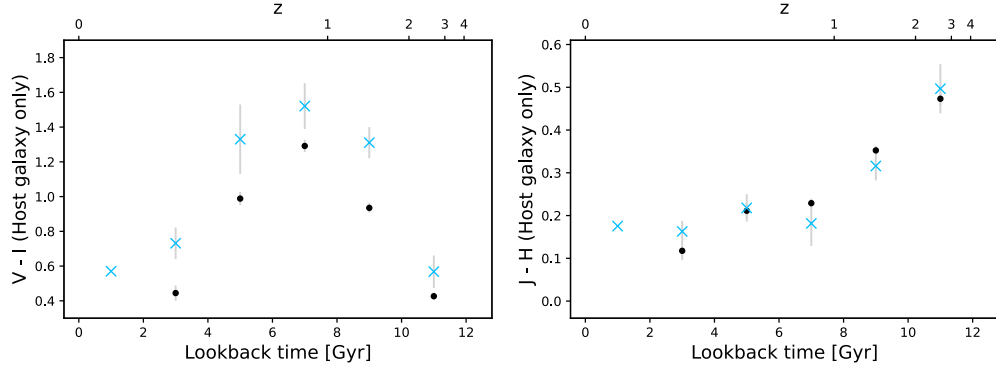


Figure 6.7: Optical $V - I$ (left) and infrared $J - H$ (right) colour vs look back time for the X-ray detected active galaxies and matched control galaxies in the CANDELS-UDS imaging region. X-ray bright active galaxies are denoted by blue crosses and corresponding matched control galaxies are shown as black points. Galaxies are averaged in bins of 2Gyrs with error bars being the standard error on the mean. Look back times are calculated based on the redshift, and corresponding redshifts are shown on the top x-axis of the plots. Magnitudes are apparent magnitudes and are drawn from the Sérsic component in a combined two component Sérsic + PSF fit to the active galaxies.

emission dominates in the total emission of the galaxy.

6.5.4 Host galaxy comparisons

We found evidence that AGN emission can be separated out from host galaxy light in active galaxies (Section 6.5.3). Using the output of the two component fitting to active galaxies, we compare the optical and infrared colours of the AGN host galaxies to a matched control set of inactive galaxies over cosmic time (Figure 6.7). Examining how the host colours change over cosmic time, we find the optical colour of X-ray AGN host galaxies are significantly redder than that of the control galaxies at a given epoch. Comparisons of the infrared colour however does not find significant differences in the overall colour of active and control galaxies. This result is in contrast to the similar measure made in Figure 6.2, where a singular Sérsic model was fit to the data and found that active galaxies as a whole had similar colours compared to matched controls.

In Figure 6.8 we examine the host colours as a function of morphology. Inspecting the disk-type galaxies, we note that the host galaxies of X-ray bright AGN appear redder in both optical and infrared colours compared to control galaxies. However, when

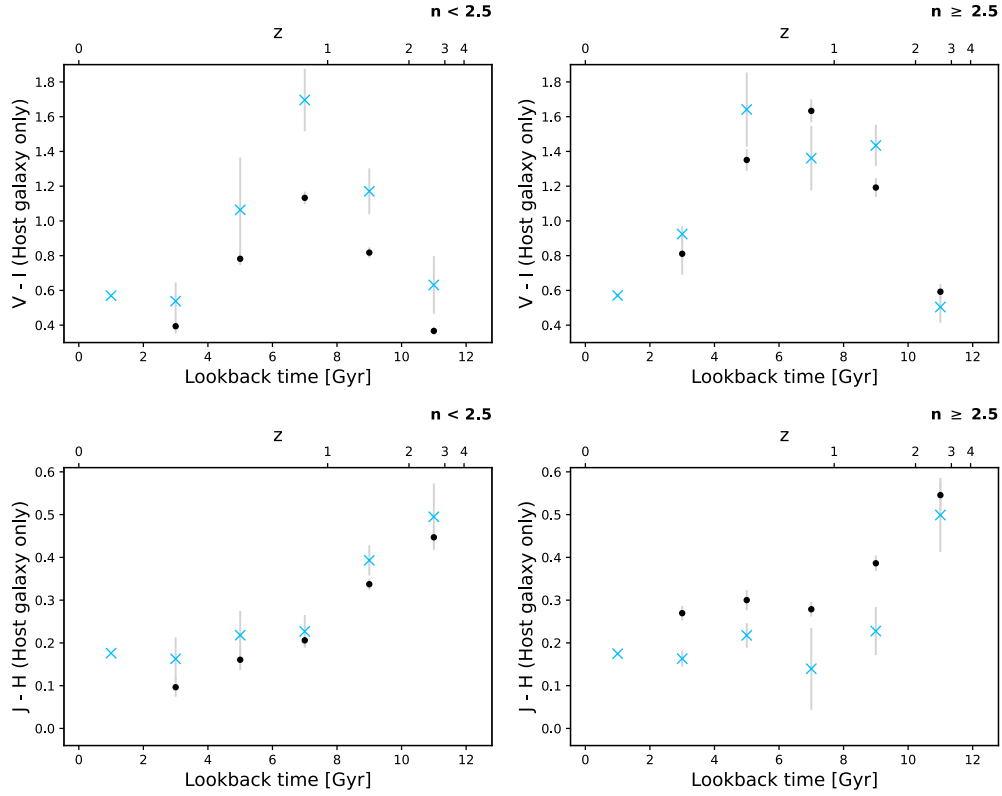


Figure 6.8: Optical ($V - I$) and infrared ($J - H$) colour vs look back time for X-ray bright active galaxies and matched control galaxies. Galaxies are split based on their Sérsic index (n) as a morphology measure, with disk type galaxies ($n < 2.5$) in the first column and spheroidal galaxies ($n \geq 2.5$) in the second column. X-ray detected AGN are shown as blue crosses and corresponding control galaxies are black points. Galaxy colours are averaged in bins of 2Gyrs with error bars being the standard error on the mean. Galaxies in these samples are drawn from the space-based CANDELS field. For active galaxies, measured magnitudes are apparent magnitudes of the point-source subtracted AGN host galaxy and the multi-band, two component fits are used to derived Sérsic indices where values are constant over wavelength. For control galaxies, measured magnitudes are apparent magnitudes from a single Sérsic profile to space based imaging and Sérsic indices are from the same model where values are constant over wavelength.

examining the spheroidal population, we find mixed results. Comparison of optical colours finds no consistent trends between X-ray AGN hosts and controls, but infrared colour comparisons are opposite to those observed in the disk-type population, with spheroidal host galaxies showing bluer colours compared to control galaxies across cosmic time. Finally, again we note that the colours observed in the AGN host galaxies are significantly different compared to measures of the overall active galaxy system (Figure 6.4) where differences between active and control galaxy colours are less distinct.

6.6 Conclusions

In this research we investigate how observations of active galaxies differ from those of inactive galaxies and whether these differences are associated with the AGN environment or host galaxy. We first match active galaxies to inactive galaxies on stellar mass, radius and redshift to form a control group, and by taking the same measurements on active and control galaxies we find a mix of differences in both active galaxy environment and host properties, some of which may be dependant on the AGN detection method.

We first find that AGN exist in different environments when splitting active galaxies by detection method (6.1). X-ray bright active galaxies are preferentially found in denser environments compared to matched inactive galaxies, but otherwise show a similar evolution of environment over cosmic time. Inspecting this same property for variability detected active galaxies however, finds they have a different cosmic evolution with environment compared to matched control galaxies. Here the environmental density of the active galaxies does not show any obvious trends over look back time, but the variability detected matched control galaxies show a similar evolution as the X-ray group. These results suggest that the triggering of X-ray bright AGN may be linked to the wider environment of the active galaxies, but the incidence of variability detected galaxies seem to be stochastic in nature.

In order to assess how the properties of active galaxies differ to those of inactive galaxies, we took a comparison of the optical and infrared colour evolution of the active and control groups (Figure 6.2). No significant differences between optical or infrared colours of either active group or their control galaxies were found, however we do note that at the 4000\AA break (≈ 1 and ≈ 2 in the optical and infrared colours respectively) we find X-ray bright sample appear redder than the variability detected sample, and this result remains true when inspecting colours of galaxy subgroups based on hardness ratio and variability band (Figure 6.3). This colour difference between samples can be explained by the high mass nature of the X-ray active galaxies compared to the variability detected galaxies, where higher mass galaxies tend to have larger passive fractions (e.g. [Krishnan et al., 2020](#)).

Further analysis shows that the colour evolution of active galaxies changes depending on morphological type (Figure 6.4). Disk-type X-ray bright AGN, for example, appear

slightly redder in both colours studied compared to control galaxies, but no consistent differences are observed between variability detected galaxies and corresponding controls. For the spheroidal sample, the optical colour of both X-ray and variability detected AGN are found to be bluer than matched control galaxies where comparisons in the infrared show no consistent differences. Splitting this same comparison into the subgroups (Figure 6.5) finds a clear distinction that X-ray soft and *J*-band variables are consistently bluer than X-ray hard and *K*-band variable galaxies. The magnitude of this difference increases at the 4000Å break in the X-ray sample, but remains consistent in the variability detected sample for all colour combinations studied.

Finally, we present preliminary research into the host properties of X-ray detected AGN. This work was restricted to the X-ray sample, as the number of variability detected active galaxies that had the high resolution imaging required for this technique to work was too small for robust conclusions to be drawn. To inspect the host properties of active galaxies, a combined two component, Sérsic + point source profile of the galaxies was taken such that host emission could be separated from the AGN. This two component analysis was largely successful on X-ray bright active galaxies (Figure 6.6), where comparisons of the infrared and X-ray luminosity improve significantly, becoming well correlated with the addition of a PSF component when fitting. Interestingly, host properties were found to differ significantly from controls galaxies, with mean optical colours appearing redder than controls at a given epoch. Further differences are found when splitting galaxies based on morphology, with disk-type host galaxies appearing redder than matched controls in both the optical and IR colour but spheroidal hosts showing no correlation with controls in the optical, but appearing bluer than controls in the IR. These preliminary results illustrate the need for AGN-host galaxy decomposition in determining accurate properties for the host galaxies AGN exist in, as well as allowing for if and how these observations may change depending on how a given AGN is detected.